

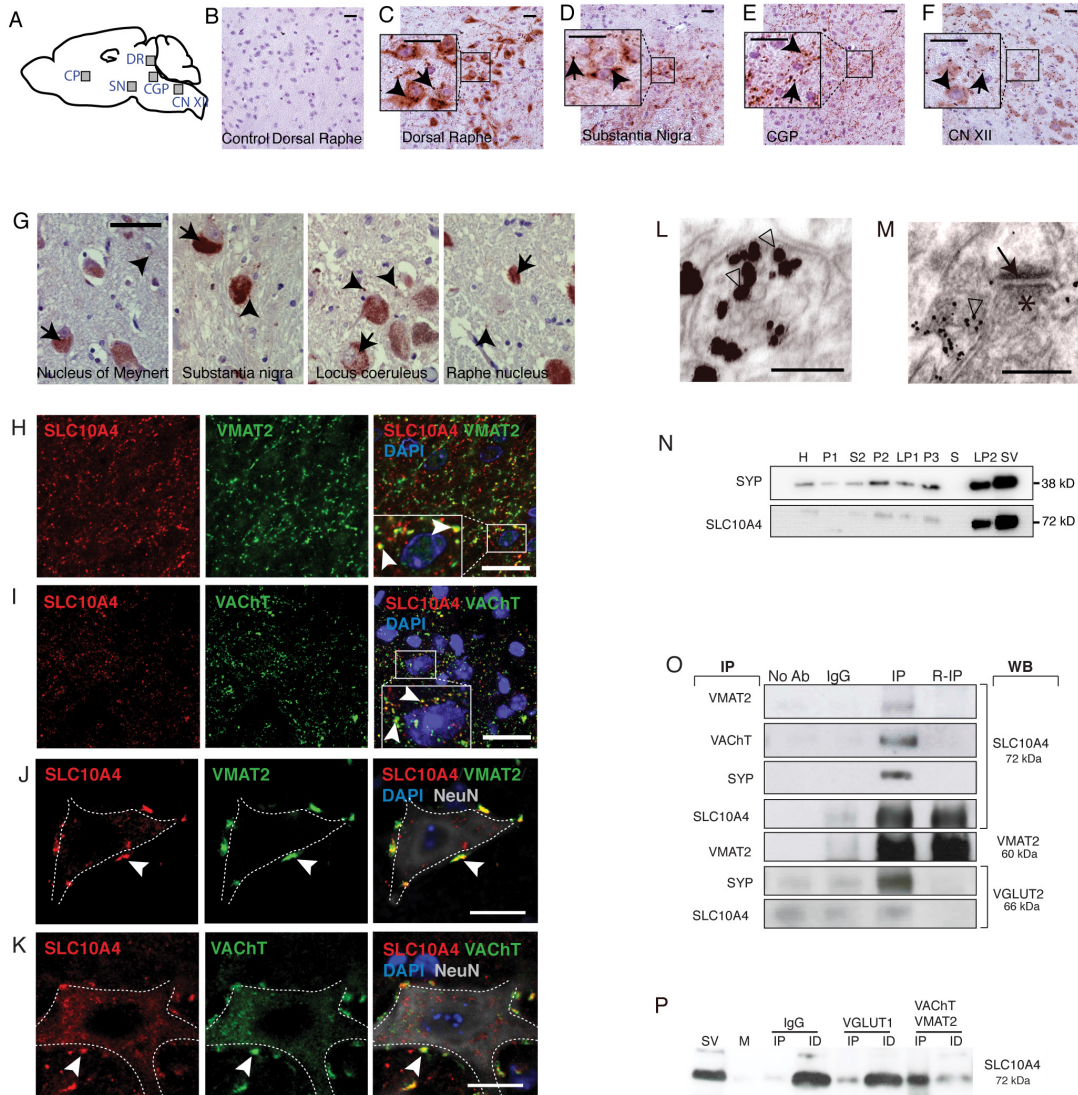
# SLC10A4 Is a Vesicular Aminergic-Associated Transporter Modulating Dopamine Homeostasis

## *Supplemental Information*

### **Table of Contents**

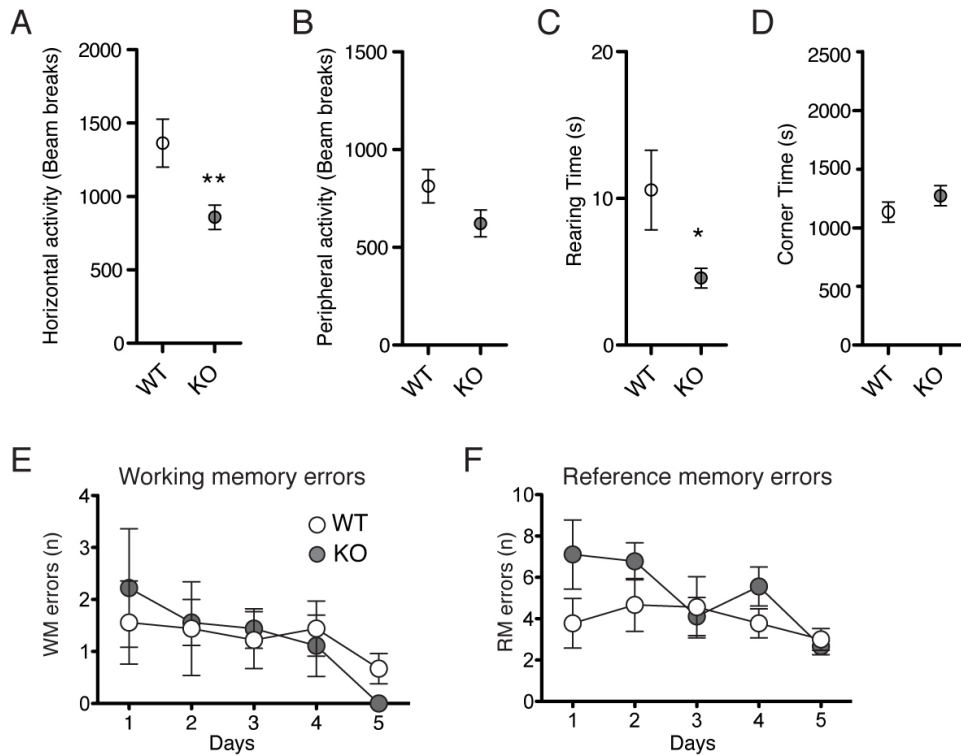
Figure S1. SLC10A4 protein expression in mouse and human brain and vesicular co-localization analysis .....	3
Figure S2. Basal behavior examination in Slc10a4 null mice.....	5
Figure S3. Behavior analysis after administration of drugs interfering with monoaminergic signaling .....	6
Table S1. Multivariate concentric square field behavior analysis .....	8
Table S2. Monoamine and acetylcholine brain tissue levels.....	9
Table S3. <i>In vivo</i> amperometry recordings of dopamine release and reuptake in the striatum and the influence of blocking VMAT2 with reserpine.....	10
Supplemental Methods and Materials .....	12
SLC10A4 Null Mutant and tgNSE-SLC10A4 Mice.....	12
Antibodies.....	13
Tissue Preparation for Histology.....	13
RNA In Situ Hybridization.....	14
Immunohistochemistry .....	15
Electron Microscopy .....	15
Western Blot.....	16
Synaptic Vesicle Preparations.....	16
Co-IP and IP-ID.....	17
Synaptic Vesicle Dopamine Uptake Assay .....	17
Acridine Orange Measurements .....	18
Stimulated Emission Depletion Microscopy and Sample Preparation .....	18
Proximity Ligation Assay.....	19
Reverse Transcription-Quantitative PCR.....	20

Table S4. Primers for RT-qPCR.....	21
HEK-293 Uptake Studies .....	21
Monoamine and Acetylcholine Measurement .....	22
Chronoamperometric <i>in vivo</i> Measurement of Dopamine Release, Reuptake and Clearance ...	23
Basal Behavioral Analysis.....	24
Behavior Analysis with Pharmacological Treatments.....	26
SLC10A4 Expression in Human Brain Autopsy Samples .....	27
Statistical Analysis .....	27
Supplemental References .....	29



**Figure S1. SLC10A4 protein expression in mouse and human brain and vesicular co-localization analysis.** (A) Schematic illustration of brain regions analyzed for SLC10A4 immunolabeling in sagittal adult mouse brain sections. (C-F) Immunohistochemistry analysis for SLC10A4 demonstrates immunopositive staining (brown) at cell-body surfaces (arrowhead) and non-cellular puncta (arrow) in dorsal raphe nucleus (C), substantia nigra (D), central gray of pons (E) and cranial nerve XII (F). Control without primary SLC10A4 antibody (B). (G) Human brain tissue sections from regions containing cholinergic (nucleus of Meynert), dopaminergic (substantia nigra), noradrenergic (locus coeruleus) or serotonergic neurons (raphe nucleus) showed SLC10A4 immunopositive signals (brown) in cellbodies (arrows) as well as in independent puncta (arrowheads). (H-K) Immunofluorescence showing co-localization (arrowheads) of SLC10A4 (red) and SLC18A2 (VMAT2, green: H, J) or SLC18A3 (VACHT, green: I, K) in the striatum (H-I) and spinal cord (J-K). Stippled line delineates a NeuN positive (gray) presumable motor neuron (J-K), DAPI (blue) labeled cell nuclei. 64% of the SLC10A4

immunolabeled terminals co-localized with VMAT2 ( $n = 991$ , 8 sections) and 26% co-localized with VACHT ( $n = 1364$ , 6 sections) in the lumbar spinal cord and 22% of the SLC10A4 immunolabeled terminals co-localized with VMAT2 ( $n = 387$ , 2 sections) and 41% co-localized with VACHT ( $n = 1274$ , 6 sections) in the caudate putamen. **(L)** Electron microscopy revealed SLC10A4 immunolabeling in vesicle containing cellular domains, often in direct association with vesicle membranes (open arrows) of symmetrical synapses, identified by the similar thickness of electron-dense regions at the presynaptic and the postsynaptic plasma membranes. **(M)** SLC10A4 immunolabeling was found in cellular domains rich in vesicles and tubular-like membrane compartments (open arrows), but not in asymmetrical synapses, recognized by their accumulation of vesicles in the presynaptic cytoplasm (asterisk) and their electron-dense postsynaptic density (arrow). **(N)** Western blot experiments showed that SLC10A4 protein was enriched together with the synaptic vesicle protein synaptophysin (SYP) throughout the purification steps of a rat brain vesicle preparation (according to (1)). **(O)** Immunoprecipitation (IP) of mouse brain synaptic vesicles with antibodies against VMAT2, VACHT, SYP, SLC10A4 or VGLUT2. ProteinG Magnetic beads were incubated with purified vesicles under different conditions; without antibody (No Ab), unspecific IgG (IgG), dissociated RIPA treated vesicles (R-IP) or vesicles with the indicated antibodies (IP). SLC10A4 (72 kDa) could be detected in the IP fractions for VMAT2, VACHT and SYP, as well as in the IP and R-IP fractions for SLC10A4. Similarly, VMAT2 could be detected in the IP and R-IP fractions for VMAT2. VGLUT2 could be detected in the IP fraction for SYP but not for SLC10A4. **(P)** Detection of SLC10A4 in samples immunodepleted (ID) with IgG, VGLUT1 or a combination of anti-VMAT2 and anti-VACHT. SLC10A4 was detected in the IP and ID fractions containing equivalent amounts of vesicular protein. The ratios of band intensity between the IP and ID fractions were: for IgG- 1:36.5, VGLUT1- 1:7.6 and for VMAT2/VACHT- 1:0.2. Scale bars: 15  $\mu\text{m}$  (**A-K**), 201 nm (**L**), 326 nm (**M**).



**Figure S2. Basal behavior examination in *Slc10a4* null mice.** (A-D) Spontaneous basal activity recorded in locomotor boxes for 40 minutes revealed a slightly hypoactive behavior in KO mice compared to WT littermate controls ( $n = 44$  per genotype). KO mice displayed a lower total horizontal activity (A,  $p = 0.007$ ) and spent less time rearing (B,  $p = 0.03$ ), while no significant differences were observed in the total peripheral activity (C,  $p = 0.08$ ) and time spent in corners (D,  $p = 0.6$ ). (E-F) Radial arm maze was used to evaluate memory, where KO and WT control mice ( $n = 10$ /genotype) did not significantly differ in the number of working memory (WM) errors (E,  $p = 0.86$ ,  $n = 9$ /genotype) or reference memory (RM) errors (F,  $p = 0.06$ ,  $n = 9$ /genotype). Student's  $t$ -test (A-D) and two-way ANOVA with Bonferroni post hoc test (E-F) were used for statistical comparison. Error bars indicate SEM,  $*p < 0.05$ ,  $**p < 0.01$ .

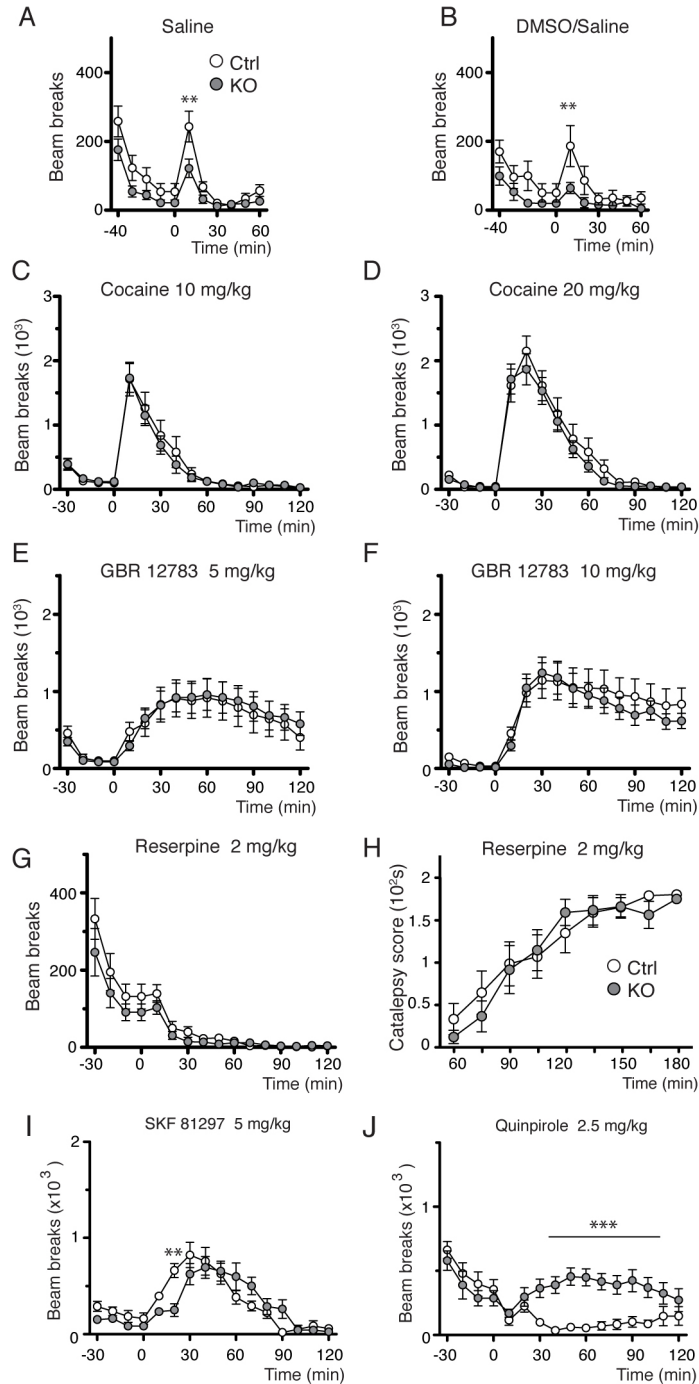


**Figure S3. Behavior analysis after administration of drugs interfering with monoaminergic signaling.** (A-B) Locomotor activity recorded for SLC10A4 KO mice (gray) and WT littermate controls (white) after administration of vehicle; Saline (A) and DMSO (5% in saline) (B). SLC10A4 WT mice responded with an initially higher locomotor activity after vehicle injection compared to KO mice (A:  $p = 0.03$ ,  $p < 0.01$  10 min after injection), (B:  $p = 0.1$  ( $p < 0.01$  10 min after injection)). (C-D) Administration of cocaine (10 and 20 mg/kg) resulted in an increased

activity in both KO and control mice that did not differ between genotypes ( $n = 16/\text{genotype}$ , **C**:  $p = 0.8$ , **D**:  $p = 0.5$ ). (**E-F**) Administration of specific DAT inhibitor GBR12783 (5 and 10 mg/kg) resulted in a similar response between genotypes for both doses ( $n = 16/\text{genotype}$ , **E**:  $p = 0.9$ , **F**:  $p = 0.7$ ). (**G-H**) Administration of VMAT2 inhibitor reserpine (2 mg/kg) resulted in a similarly decreased locomotor activity in both KO and control mice ( $n = 16/\text{genotype}$ ,  $p = 0.7$ ) and the mice reached a cataleptic state after similar time periods (**H**,  $p = 0.5$ ). (**I**) Administration of D1-like dopamine receptor agonist SKF81297 5 mg/kg resulted in a significantly slower response in SLC10A4 KO mice compared to controls ( $p = 0.5$ ). (**J**) Administration of the D2-like dopamine receptor agonist quinpirole caused a significant difference between the genotypes in their locomotor response for the dose of 2.5 mg/kg ( $p = 0.003$ ). Cocaine, GBR 12783, reserpine and tranylcypromine ( $n = 16/\text{genotype}$ , respectively), SKF 81297 and quinpirole ( $n = 9/\text{genotype}$ , respectively). Two-way ANOVA with Bonferroni post hoc test was used for statistical analysis, error bars indicate SEM, \*\* $p < 0.01$ , \*\*\* $p < 0.001$ .

**Table S1. Multivariate concentric square field (MCSF) behavior analysis.** The MCSF test was used to analyze exploration, risk assessment, risk taking, shelter seeking, and approaching and avoidance behavior. SLC10A4 KO and WT control littermates ( $n = 9/\text{genotype}$ ) were scored for latency (LAT), frequency (FRQ), duration (DUR) and duration/frequency (DUR/FRQ) for each area in the MCSF: Centre, Central circle, Corridor a-c, dark room, hurdle, bridge, slope 1-2. Data was analyzed with Student's *t*-test for each parameter indicated in the table. The MCSF test and the functional interpretation of the various parameters have been described in details elsewhere (2).

PARAMETERS	WT Control	Slc10a4 KO	T-test (2:2)
LAT LEAVE	227.8 ± 54.5	228.5 ± 34.3	0.99
LAT DCR	99.9 ± 43.0	115.7 ± 49.8	0.81
LAT SLOPE	280.8 ± 58.8	232.4 ± 41.6	0.51
LAT BRIDGE	259.1 ± 44.0	249.5 ± 48.5	0.89
LAT HURDLE	67.8 ± 46.5	68.0 ± 37.1	1.00
LAT CTRCI	36.0 ± 26.6	146.6 ± 73.2	0.17
FRQ CENTRE	6.6 ± 1.9	11.7 ± 3.3	0.20
FRQ DCR	1.4 ± 0.6	1.9 ± 0.8	0.66
FRQ SLOPE	14.4 ± 1.8	17.9 ± 3.0	0.34
FRQ BRIDGE	9.3 ± 1.3	12.0 ± 2.2	0.31
FRQ HURDLE	0.3 ± 0.2	0.7 ± 0.3	0.43
FRQ CTRCI	1.0 ± 0.4	2.8 ± 1.1	0.14
FRQ TOTCORR	12.3 ± 3.3	18.0 ± 3.2	0.24
DUR CENTRE	100.4 ± 32.0	176.7 ± 49.8	0.22
DUR DCR	21.3 ± 14.6	27.1 ± 12.2	0.76
DUR SLOPE	233.7 ± 45.2	209.2 ± 38.1	0.68
DUR BRIDGE	442.5 ± 104.0	224.7 ± 43.5	0.07
DUR HURDLE	152.6 ± 114.0	176.9 ± 124.5	0.89
DUR CTRCI	1.9 ± 1.1	4.3 ± 1.3	0.18
DUR TOTCORR	243.9 ± 69.3	376.0 ± 81.7	0.24
DUR/FRQ CENTRE	17.4 ± 2.8	17.9 ± 5.2	0.93
DUR/FRQ DCR	12.2 ± 5.0	17.1 ± 8.3	0.65
DUR/FRQ SLOPE	15.3 ± 1.9	11.8 ± 0.9	0.14
DUR/FRQ BRIDGE	46.0 ± 8.8	19.1 ± 1.6	0.013*
DUR/FRQ HURDLE	435.5 ± 67.0	207.7 ± 74.3	0.13
DUR/FRQ TOTCORR	19.9 ± 3.8	25.7 ± 8.5	0.54
TOTACT	45.44 ± 1.4	64.89 ± 1.6	0.38

**Table S2. Monoamine and acetylcholine brain tissue levels.** Quantification of monoamine content in the striatum of SLC10A4 KO mice and WT control mice was done by high-performance liquid chromatography. Norepinephrine (NE), dopamine (DA) and serotonin (5-HT) concentrations were all significantly reduced in both caudate putamen and nucleus accumbens in SLC10A4 KO mice (gray) compared to control (ng/g wet tissue,  $n = 20$ /genotype). In addition, KO animals had reduced levels of the DA metabolite 3,4-dihydroxyphenylacetic acid (DOPAC) but not of homovanillic acid (HVA), compared to controls. DA turnover ratios were calculated: [DOPAC]/[DA], [HVA]/[DA] and ([DOPAC]+ [HVA])/[DA]), showing increased DA turnover ratios in both regions of SLC10A4 KO mice compared to WT controls. Acetylcholine (ACh) and choline tissue levels measured in a combined striatum and midbrain preparation were determined by a commercially available ACh/choline assay kit (ab65345, Abcam). Choline concentration was reduced in KO brain tissue whereas ACh levels did not differ significantly. Statistical significance was analyzed with Student's two-tailed  $t$ -test ( $p$ -values indicated). Data are presented as mean  $\pm$  SEM.

	Control	KO	% of ctrl	p-value
<b>Caudate Putamen</b> (n=20)				
NE	0.23 $\pm$ 0.02	0.11 $\pm$ 0.01	48	< 0.001
DOPAC	3.68 $\pm$ 0.26	2.27 $\pm$ 0.12	59	< 0.001
DA	9.68 $\pm$ 0.66	3.43 $\pm$ 0.31	37	< 0.001
HVA	2.16 $\pm$ 0.10	1.98 $\pm$ 0.08	116	0.176
5-HT	0.48 $\pm$ 0.03	0.32 $\pm$ 0.02	67	< 0.001
(DOPAC+HVA)/DA	0.67 $\pm$ 0.06	1.51 $\pm$ 0.21	166	< 0.001
DOPAC/DA	0.42 $\pm$ 0.04	0.80 $\pm$ 0.10	190	0.002
HVA/DA	0.24 $\pm$ 0.02	0.71 $\pm$ 0.11	296	< 0.001
<b>Nucleus Accumbens</b> (n=20)				
NE	0.20 $\pm$ 0.02	0.15 $\pm$ 0.01	75	0.026
DOPAC	1.91 $\pm$ 0.21	1.27 $\pm$ 0.12	58	0.012
DA	2.09 $\pm$ 0.31	0.79 $\pm$ 0.14	61	< 0.001
HVA	1.20 $\pm$ 0.13	1.07 $\pm$ 0.09	84	0.411
5-HT	0.39 $\pm$ 0.04	0.27 $\pm$ 0.03	69	0.012
(DOPAC+HVA)/DA	1.99 $\pm$ 0.32	4.05 $\pm$ 0.50	154	0.001
DOPAC/DA	1.22 $\pm$ 0.20	2.12 $\pm$ 0.25	161	0.007
HVA/DA	0.77 $\pm$ 0.12	1.93 $\pm$ 0.26	199	< 0.001
<b>Striatum/Midbrain</b>				
ACh (n=8)	0.13 $\pm$ 0.02	0.11 $\pm$ 0.02	83	0.43
Choline (n=10)	0.96 $\pm$ 0.06	0.70 $\pm$ 0.07	73	0.02

**Table S3. *In vivo* amperometry recordings of dopamine release and reuptake in the striatum and the influence of blocking VMAT2 with reserpine.** *In vivo* chronoamperometry recordings of induced dopamine (DA) release and reuptake in the striatum (anterior-posterior +1.1 mm; medial-lateral  $\pm$  1.5 mm, dorso-ventral -3.2 mm from bregma) after KCl evoked release (upper left table), KCl evoked release after i.p. reserpine treatment (upper right table), exogenous DA evoked clearance (bottom left table) and exogenous DA evoked clearance after i.p. reserpine treatment (bottom right table). The following parameters were analyzed for KCl evoked release and reuptake for five consecutive ejections: Amplitude, Peak Area, T-rise, T-80 and Tc, and for exogenous clearance amplitudes of 45, 22 and 5  $\mu$ M DA, respectively; Peak Area, T-rise, T-80 and Tc. For definitions of each parameter see Supplemental Methods & Materials section. Statistical significance (*p*-values) and the number of animals (*n*) are indicated in the table. Two-way ANOVA with Bonferroni post hoc test was used for statistical analysis.

<b>Caudate Putamen</b>				<b>Caudate Putamen - post reserpine treatment (i.p.)</b>					
		Mean values		2way ANOVA	Bonferroni			2way ANOVA	Bonferroni
		WT	KO			WT	KO		
<b>Evoked release and reuptake</b>									
<b>Amplitude</b>									
KCl ejection	DA conc ( $\mu$ M)	DA conc ( $\mu$ M)							
1	3.99	5.15		$P > 0.05$	1	1.11	2.99		$P < 0.01$
2	2.51	2.90		$P > 0.05$	2	0.85	1.82		$P > 0.05$
3	1.87	2.44		$P > 0.05$	3	0.50	1.41		$P > 0.05$
4	1.85	2.45		$P > 0.05$	4	0.43	1.38		$P > 0.05$
5	1.51	2.31		$P > 0.05$	5	0.41	1.30		$P > 0.05$
	(n=5)	(n=5)		$P=0.54$		(n=4)	(n=3)		$P=0.06$
<b>Peak Area</b>									
KCl ejection	Area ( $\mu$ M $\cdot$ sec)	Area ( $\mu$ M $\cdot$ sec)			KCl ejection	Area ( $\mu$ M $\cdot$ sec)	Area ( $\mu$ M $\cdot$ sec)		
1	96.84	374.87		$P < 0.001$	1	64.47	266.76		$P < 0.01$
2	44.70	87.76		$P > 0.05$	2	23.75	64.68		$P > 0.05$
3	32.62	72.45		$P > 0.05$	3	12.92	36.18		$P > 0.05$
4	34.14	62.49		$P > 0.05$	4	6.31	40.85		$P > 0.05$
5	28.84	48.44		$P > 0.05$	5	8.61	37.46		$P > 0.05$
	(n=5)	(n=5)		$P=0.06$		(n=4)	(n=3)		$P=0.09$
<b>T rise</b>									
KCl ejection	t (sec)	t (sec)			KCl ejection	t (sec)	t (sec)		
1	9.80	21.00		$P < 0.05$	1	23.75	31.67		$P > 0.05$
2	10.20	13.00		$P > 0.05$	2	20.75	16.33		$P > 0.05$
3	9.90	12.70		$P > 0.05$	3	14.50	10.67		$P > 0.05$
4	10.30	11.90		$P > 0.05$	4	9.50	11.67		$P > 0.05$
5	9.80	11.30		$P > 0.05$	5	15.25	11.00		$P > 0.05$
	(n=5)	(n=5)		$P=0.17$		(n=4)	(n=3)		$P=0.95$
<b>T 80</b>									
KCl ejection	t (sec)	t (sec)			KCl ejection	t (sec)	t (sec)		
1	22.80	63.60		$P < 0.001$	1	46.50	105.00		$P < 0.05$
2	16.10	23.70		$P > 0.05$	2	31.00	42.67		$P > 0.05$
3	17.20	28.60		$P > 0.05$	3	27.00	37.00		$P > 0.05$
4	14.80	20.10		$P > 0.05$	4	13.75	40.33		$P > 0.05$
5	18.00	17.70		$P > 0.05$	5	18.75	39.67		$P > 0.05$
	(n=5)	(n=5)		$P=0.02$		(n=4)	(n=3)		$P=0.13$
<b>Tc</b>									
KCl ejection	Rate ( $\mu$ M/s)	Rate ( $\mu$ M/s)			KCl ejection	Rate ( $\mu$ M/s)	Rate ( $\mu$ M/s)		
1	-0.18	-0.12		$P > 0.05$	1	-0.023	-0.047		$P > 0.05$
2	-0.16	-0.17		$P > 0.05$	2	-0.037	-0.039		$P > 0.05$
3	-0.12	-0.18		$P > 0.05$	3	-0.035	-0.052		$P > 0.05$
4	-0.13	-0.19		$P > 0.05$	4	-0.036	-0.039		$P > 0.05$
5	-0.094	-0.20		$P > 0.05$	5	-0.038	-0.041		$P > 0.05$
	(n=5)	(n=4)		$P=0.62$		(n=4)	(n=3)		$P=0.76$

Table S3, *continued*

<i>Caudate Putamen</i>				<i>Caudate Putamen - post reserpine treatment (l.p.)</i>				
	Mean values		2way ANOVA	Bonferroni	Mean values		2way ANOVA	Bonferroni
	WT	KO			WT	KO		
Evoked clearance (exogenous dopamine)								
<i>Peak Area</i>					<i>Peak Area</i>			
<i>DA ejection Amp. (µM)</i>	<i>Area (µM*sec)</i>	<i>Area (µM*sec)</i>			<i>DA ejection Amp. (µM)</i>	<i>Area (µM*sec)</i>	<i>Area (µM*sec)</i>	
45	1380.19	1753.33		P > 0.05	45	2183.55	2168.21	P > 0.05
22	559.56	844.50		P > 0.05	22	1487.57	901.326	P > 0.05
5	109.67	176.72		P > 0.05				
	(n=4)	(n=6)	P=0.07			(n=3)	(n=3)	P=0.40
<i>T rise</i>					<i>T rise</i>			
<i>DA ejection Amp. (µM)</i>	<i>t (sec)</i>	<i>t (sec)</i>			<i>DA ejection Amp. (µM)</i>	<i>t (sec)</i>	<i>t (sec)</i>	
45	12.00	11.44		P > 0.05	45	9.11	10.50	P > 0.05
22	11.50	12.38		P > 0.05	22	10.00	9.67	P > 0.05
5	10.46	13.77		P > 0.05				
	(n=4)	(n=6)	P=0.57			(n=3)	(n=3)	P=0.75
<i>T 80</i>					<i>T 80</i>			
<i>DA ejection Amp. (µM)</i>	<i>t (sec)</i>	<i>t (sec)</i>			<i>DA ejection Amp. (µM)</i>	<i>t (sec)</i>	<i>t (sec)</i>	
45	37.33	51.17		P > 0.05	45	75.89	76.67	P > 0.05
22	33.42	49.17		P > 0.05	22	73.00	54.86	P > 0.05
5	26.13	43.60		P < 0.05				
	(n=4)	(n=6)	P=0.0005			(n=3)	(n=3)	P=0.65
<i>Tc</i>					<i>Tc</i>			
<i>DA ejection Amp. (µM)</i>	<i>Rate (µM/s)</i>	<i>Rate (µM/s)</i>			<i>DA ejection Amp. (µM)</i>	<i>Rate (µM/s)</i>	<i>Rate (µM/s)</i>	
45	-1.56	-0.91		P < 0.05	45	-0.75	-0.77	P > 0.05
22	-0.71	-0.47		P > 0.05	22	-0.34	-0.49	P > 0.05
5	-0.22	-0.12		P > 0.05				
	(n=4)	(n=6)	P=0.02			(n=3)	(n=3)	P=0.66

## Supplemental Methods and Materials

### SLC10A4 Null Mutant and tgNSE-SLC10A4 Mice

The *Slc10a4* null mutant (KO) mouse line was generated by Texas A&M Institute for Genomic Medicine TIGM (TX, USA, <http://www.tigm.org/>). The coding region of the three *Slc10a4* exons was deleted in embryonic stem cells by genetrapping using a  $\beta$ -geo Puro cassette (Figure 2A) (genomic sequence chr5:73,007,069-73,012,380, [http://web.tigm.tamu.edu/cgi-bin/new\\_tigmdatabase.cgi](http://web.tigm.tamu.edu/cgi-bin/new_tigmdatabase.cgi)). The *Slc10a4* KO allele was verified by Southern blot after *SacI* digestion. Heterozygous *Slc10a4* mice on a 129/SvEvBrd background were maintained on a C57/BL6 background. Male and female mice between 6 and 24 weeks were used for molecular and behavioral tests. *Slc10a4* KO mice were investigated with wild type littermates as controls, if not stated otherwise. For genotyping the following primers were used: SLC10A4 null mutant: forward 5'- CAGGTAAAGGGACCACAGG, reverse 5'-ACACCGGCCTTGTATTTGTAGC and wild type control: forward 5'-GGAAAGACATGGCTGACTCTG, reverse 5'-CACGCGGTTGTATTTGTAGC.

Transgenic *NSE-Slc10a4* (NSE-SLC10A4) mice: the full length *Slc10a4* cDNA (RIKEN clone E130304D01, Source BioScience, Nottingham, UK) was inserted downstream of the rat neuron specific enolase (*NSE*, *enolase 2*) promoter as previously described (3). The pNSE-Ex4 rat vector was kindly provided by Dr. J. Gregor Sutcliffe (Dept. of Molecular Biology, The Scripps Research Institute, La Jolla, USA). Briefly, HindIII-linkers were attached to *Slc10a4* cDNA by polymerase chain reaction (PCR) and cloned into the HindIII site of the pNSE-Ex4 vector. Correct insert orientation was verified by PCR using the primers: 5'-CTCTTGTCACCCAAGGAGA and 5'-GACCGGGACTAGAGGTGACA. Linearized *NSE-Slc10a4* construct was purified and introduced to the genome by pronuclear injection at Uppsala University Transgenic Facility. Founder animals were identified by PCR (forward 5'-CTCTTGTCACCCAAGGAGA and reverse 5'-GACCGGGACTAGAGGTGACA) and bred with C57BL/6 mice. Positive founders were analyzed by in situ hybridization and western blot (WB). Heterozygous C57BL/6-Tg(NSE-*Slc10a4*) animals were used for experiments and are here referred to as NSE-SLC10A4.

All mice were kept according to the guidelines of Swedish regulation and European Union legalization (ethical permits C79/9,2009-03-27; C256/8 2008-10-31; C3/9 2009-01-30; C143/9 2009-04-29; C142/9 2009-05-29; C65/10 2010-03-26; C240/10 2010-09-24).

## **Antibodies**

Antibodies for immunohistochemistry (IHC), WB, co-immunoprecipitation (Co-IP), electron microscopy (EM), stimulated emission depletion microscopy (STED) and proximity-ligation assay (PLA) were used in the following dilutions: Rabbit anti-SLC10A4 (HPA028835, Sigma-Aldrich, St. Louis, USA) IHC 1:2000, WB 1:1000, STED, PLA 1:1000; Mouse anti-synaptophysin (Sigma-Aldrich) IHC 1:400, WB 1:1000; Guinea pig anti-VACHT (Millipore, Billerica, USA) IHC 1:500, WB 1:500, STED, PLA 1:100; Goat anti-VACHT (Santa Cruz Biotechnology, Santa Cruz, USA) IHC, STED, PLA 1:50; Goat anti-VMAT2 (Santa Cruz Biotechnology) IHC 1:50; Goat anti-VMAT2 (Abcam, Cambridge, UK) STED, STED, PLA 1:100; Guinea pig anti-VMAT2 (El Mestikawy, S. Douglas Mental Health University Institute, Montreal, Canada, (4)) WB 1:500, PLA, STED 1:50; Rabbit anti-SLC10A4 (Geyer J., University of Justus-Liebig, Giessen, Germany, (5)) IHC 1:1000, EM 1:1000; Guinea pig anti-VGLUT2 (Abcam, Cambridge, UK) WB, 1:10000. Antibodies for co-IP were used at a concentration of 2 µg per 100 µg of total protein. For the IP-immunodepletion (ID) experiments, the following antibodies from Synaptic Systems (Göttingen, Germany) were used: Rabbit anti-VGLUT1, Rabbit anti-VMAT2, Rabbit anti-VACHT, along with the Rabbit anti-SLC10A4 (Sigma) described above.

## **Tissue Preparation for Histology**

Adult mice were anaesthetized by IP injection of a 50:50 (vol/vol) mixture of Ketalar 7 µg/g bodyweight (Pfizer, Groton, CT) and Domitor 70 µg/g bodyweight (Orion, Espoo, Finland), and fixed by transcardiac perfusion with PBS followed by 4 % formaldehyde in PBS. Brain and spinal cord were dissected out and post-fixed overnight (O/N) in 4% formaldehyde in PBS. For cryo sections (10-16 µm) the tissue was cryoprotected O/N in 30% sucrose in PBS, embedded in TissueTec®, and frozen on dry ice. The sections were collected on Superfrost Plus slides (Menzel GmbH, Braunschweig, Germany) and stored at -80°C. For floating sections (60-80 µm) O/N fixed tissue was washed in PBS, embedded in 4 % agarose in PBS, sectioned by Vibratome

(Leica, Wetzlar, Germany) and dehydrated in a graded series of methanol before storage in absolute methanol in -20°C. For paraffin sections (7 µm) O/N fixed tissue was dehydrated and embedded in paraffin, cut using a cool-cut rotary microtome HM 355S (MICROM, Waldorf, Germany) and stored at 4°C. For electron microscopy experiments rodents were deeply anesthetized (adult female Sprague-Dawley rats were anesthetized with 75-100 µg/g bodyweight ketamine, 10 µg/g bodyweight xylazine, i.p and mice with Ketalar 7 µg/g bodyweight and Domitor 70 µg/g bodyweight and fixed by transcardiac perfusion. Prior to fixation with 4% paraformaldehyde, 0.05% glutaraldehyde, 0.2% picric acid in 0.1 M sodium phosphate buffer, pH 7.4, the blood was exchanged with PBS containing 0.3% sodium nitroprusside and heparin (10 U/ml). Fixation was carried out at room temperature (RT) for ~20 min at a flow rate of 20 ml/min. The striatum was dissected out, immersed in fixative O/N at 4°C and washed thoroughly with PBS before electron microscopy analysis.

### **RNA In Situ Hybridization**

RNA in situ hybridization was performed using an anti-sense probe for *slc10a4* covering nucleotides 1375-2085 (NCBI accession number NM\_173403.2). In situ hybridization was done in an RNase free environment on free-floating sections as has been described elsewhere (6). Floating sections were rehydrated by sequential dilution of methanol to PBT (PBS, 0.1% Tween-20), treated with 20 µg/ml Proteinase K (Invitrogen, Life Technologies, Carlsbad, USA), post-fixed, washed and incubated at RT in hybridization buffer (50% formamide, 5X SSC, 1% SDS, 50 µg/ml tRNA, 50 µg/ml heparin). After 2 h the hybridization buffer was replaced with 300 ng/ml DIG-labeled antisense RNA probe diluted in hybridization buffer and incubated at 65°C O/N. After three stringent washes with 0.2X SSC at 65°C for 30 min each, sections were incubated in blocking solution (Product number: 10057177103, Roche Diagnostics) at room temperature for 2 h, followed by overnight incubation with anti-DIG Fab fragments conjugated to alkaline phosphatase (Roche Diagnostics) diluted 1:5000 in blocking solution. Finally, bound probes were detected by NBT/BCIP (Roche Diagnostics) used as a substrate to alkaline phosphatase. Cryo-in situ hybridization was performed essentially as previously described (7).

## **Immunohistochemistry**

Immunohistochemistry was performed on cryocut sections as well as fixed HEK293 cells at 70% confluency transfected 24 h prior to analysis. After washing in PBS, sections were incubated for 1 h in blocking buffer (0.3% Triton X-100, 10% serum, 0.3% BSA in PBS). Antibodies (listed above) were incubated O/N in 0.1% Triton X-100, 10% serum, 0.01% sodium-azide in PBS. Secondary antibody incubation was performed after 3 washes in PBS using Alexa Fluor®488, 594 and 647 conjugated secondary antibodies (Jackson ImmunoResearch Europe LTD, UK) diluted in PBS or 0.1% Triton X-100, 10% normal serum, 0.01% sodium-azide in PBS with 4',6'-diamidino-2-phenylindole (DAPI) as nuclear counterstaining. Chromogen immunohistochemistry was performed using Vectastain Elite ABC Kit (Vector Laboratories LTD, Peterborough, UK), according to the manufacturer's protocol. As color substrate 3,3'-diaminobenzidinetetrahydrochloride (DAB) was used (Vector Laboratories LTD, Peterborough, UK). Before mounting with Mowiol, samples were washed in PBS. Fluorescent images were captured using a ZEISS LSM 510 META confocal microscope and ZEISS LSM510 image analysis software and images were adjusted for brightness and contrast using Volocity 4.1.0 software (Perkin Elmer). Samples stained with DAB were photographed using an Olympus BX61WI microscope.

## **Electron Microscopy**

Pre-embedding immunolabeling was done as described previously (8), using free-floating vibratome sections of striatum. Sections were permeabilized with 1% sodium borohydride and incubated with the primary antibody for 60 h at 4°C. After repeated rinsing and blocking, sections were incubated with Nanogold-coupled goat anti-rabbit Fab' antibody fragments (Nanoprobes Inc., Yaphank, USA) for 20 h at 4°C. Bound antibodies were fixed with 2.5% glutaraldehyde in PBS for 45 min, and nanogold particles were silver intensified for 10 to 13 min according to Burry *et al.* (9). The sections were post fixed with 1% osmium tetroxide in phosphate buffer for 20 min and bloc-stained with 0.5% aqueous uranyl acetate for 20 min. Dehydration was done by an ethanol series and propylene oxide and followed by embedding in araldite. Sections were collected on copper grids and counterstained with uranyl acetate and lead citrate.

## Western Blot

Proteins were separated on 4-15% mini-PROTEAN<sup>®</sup> TGX<sup>™</sup> precast gel (Bio-Rad Laboratories AB, Sweden) at 121 V for 1 h and transferred to a nitrocellulose membrane (Bio-Rad Laboratories AB) at 15 V for 30 min in a semi-dry electrophoretic transfer cell (Bio-Rad Laboratories AB). The membrane was blocked with 3% BSA in TBS-Tween 20 for 1 h and incubated with primary antibody in the same blocking solution for 2 h at RT, followed by four washes in TBST (50 mM Tris pH 8, 150 mM NaCl, 0.05% Tween20). The membrane was then incubated with protein A-HRP conjugate (Bio-Rad Laboratories AB) for 1 h at RT followed by washing in TBST and detection with luminol reagent.

## Synaptic Vesicle Preparations

Synaptic vesicles (SV) used for immunoprecipitation experiments, acridine orange  $\Delta$ pH measurements and dopamine (DA) uptake were enriched using a modified protocol based on Teng *et al.* (10). In brief, the striatum or whole brain from three mice (6-12 weeks old) were dissected, pooled and homogenized in 15 ml of ice-cold 0.32 M HEPES buffered sucrose (HBS) at 900 RPM with 10 up-and-down strokes of a tight fitting Teflon homogenizer. All steps were carried out below 4°C. The brain homogenate was centrifuged at 2,000 g for 10 min to pellet down cell debris, intact cells and nuclei. Supernatant was transferred to another tube and centrifuged at 15,000 g for 15 min. The “buffy coat” of the resulting pellet, here referred to as a crude synaptosomal fraction, was dissolved in 2 ml of ice-cold 0.32 M HBS and immediately transferred to a glass Teflon homogenizer containing 7 ml of deionized water to provide an osmotic shock. The suspension was homogenized at 2,000 RPM with 3 up-and-down strokes, and the osmolarity was restored after 2 min by adding 900  $\mu$ l 0.25 M HEPES pH 7.4 (KOH), 900  $\mu$ l 1 M potassium tartrate pH 7.4 (KOH) and protease inhibitor cocktail (Roche Diagnostics, Mannheim, Germany). The suspension was centrifuged at 20,000 g for 20 min and the resulting supernatant was centrifuged at 55,000 g for 60 min to remove contaminating membrane pieces and larger vesicular structures. To the resulting supernatant 100  $\mu$ l of each 0.01 M MgSO<sub>4</sub>, 0.25 M HEPES pH 7.4 (KOH) and 1M potassium tartrate pH 7.4 (KOH) was added and centrifuged at 100,000 g for 120 min. The final pellet containing small synaptic vesicles was dissolved in 300-500  $\mu$ l storage buffer or Krebs-Ringer buffer (in mM: 140 NaCl, 5 KCl, 2 MgCl<sub>2</sub>, 2 CaCl<sub>2</sub>, 10 HEPES, 6 sucrose, 10 glucose, pH 7.4) and passed 5 times through a 25 gauge needle. Vesicles

used for STED and in situ PLA were purified using a hybrid of existing protocols allowing increase purity of SV and described in detail elsewhere (11). Enrichment studies of SLC10A4 were performed using western blot on synaptic vesicles purified from both mouse and rat brain (1). Protein content was quantified by Bradford assay.

### **Co-IP and IP-ID**

Co-IP was performed on enriched synaptic vesicles equivalent of 200 µg total protein. Synaptic vesicles were incubated overnight at 4°C with 4 µg of appropriate primary antibody or normal IgG in 700 µl incubation buffer (PBS, 2 mM EDTA and 0.05% BSA). RIPA buffer (700 µl, 150 mM NaCl, 50 mM Tris, 1% Triton X-100, 0.5% sodium deoxycholate, 0.1% sodium dodecyl sulfate) treated vesicle fractions was used to check for vesicle integrity and to test for direct protein interactions. 75 µl corresponding to 1.5 mg of magnetic beads (Dynabeads, Life Technologies, Sweden) were equilibrated in 200 µl incubation buffer and added to the antibody-vesicle solution for 1 h in RT. Immune complexes were washed three times with incubation buffer and eluted in sample buffer (20% glycerol, 4% SDS and 0.05% bromophenol blue, 5% β-mercaptoethanol) at 70°C for 10 min.

IP-ID was performed with 100 µg total vesicle protein in 200 µl of incubation buffer. Enriched synaptic vesicles were immunoprecipitated with rabbit IgG, rabbit-VGLUT1, rabbit-VMAT2 & rabbit-VACHT, or rabbit-SLC10A4 in the same manner as described for co-IP. Protein equivalents from the enriched SV, the IP fractions and corresponding immunodepleted fractions were separated by SDS PAGE and SLC10A4 band was detected by western blot. The free trial version of myImageAnalysis software from Pierce (<http://www.piercenet.com/product/myimageanalysis-software>) was used to analyze the band intensities.

### **Synaptic Vesicle Dopamine Uptake Assay**

Synaptic vesicle dopamine uptake was performed by incubating 15 µg protein of freshly prepared striatal vesicles in 100 µl assay buffer (Krebs-Ringer buffer with 50 nM <sup>3</sup>HDA (Perkin Elmer, Waltham, USA) and 2 mM ATP-Mg final concentration) for 4 and 8 min at 32°C. Uptake was terminated by rapid dilution in 3 ml of ice-cold wash buffer (in mM: 10 MOPS, 100 potassium gluconate, 2 MgCl<sub>2</sub>). Non-specific uptake was determined by pre-incubating vesicles

in the presence of 200 nM reserpine for 5 minutes at 32°C prior to addition of assay buffer, as well as uptake performed on ice. The samples were filtered through Whatman GF/F filters (Whatman, Maidstone, UK) and washed with 5 ml of ice-cold wash buffer. Uptake was quantified by scintillation counting of <sup>3</sup>HDA retained in the filters. Measurements were conducted in triplicates from simultaneously prepared vesicle samples from *NSE-Slc10a4*, *Slc10a4* null mutant and WT littermate controls (4-8 preparations per genotype). Non-specific uptake (determined in the presence of reserpine) was subtracted. Data from independent experiments were combined and analyzed for statistical significance using 2-way ANOVA.

### Acridine Orange Measurements

The  $\Delta\text{pH}$  component of the electrochemical potential ( $\Delta\mu\text{H}^+$ ) over SV membranes was analyzed by the quenching of the pH sensitive dye acridine orange, where quenching of the acridine orange fluorescence reflects the generation of an inside-acidic  $\Delta\text{pH}$ . The experimental protocol was adapted from (12). In brief, synaptic vesicles (60  $\mu\text{g}$ ) enriched from *Slc10a4* KO, WT and *NSE-Slc10a4* brains were incubated with acridine orange (2.5  $\mu\text{M}$ ) in Krebs-Ringer buffer (2 ml) for 5 min at 32°C. Fluorescence measurements were performed under constant stirring at 32°C using a SPEX fluorolog 1650 0.2 m double spectrometer (SPEX Industries, Edison, NJ), excitation and emission wavelengths were set to 492 and 530 nm, respectively. Acidification was initiated by the addition of Mg-ATP (1 mM final concentration). The protonophore carbonyl cyanide m-chlorophenyl hydrazone (CCCP) was added after 5 min to validate specific acidification (12.5  $\mu\text{M}$  final concentration). Normalized fluorescent change,  $\Delta\text{F}/\text{F}$ , was used for statistical comparison between genotypes using 2-way ANOVA followed by Bonferroni's post-hoc test.  $[\Delta\text{F}]/[\text{F}] = [\text{F}_{\text{average}}(t_{-1\text{min}} - t_{0\text{min}}) - \text{F}_{\text{average}}(t_{1\text{min}} - t_{2\text{min}})] / [\text{F}_{\text{average}}(t_{-1\text{min}} - t_{0\text{min}})]$ .

### Stimulated Emission Depletion Microscopy and Sample Preparation

Synaptic vesicles equivalent to 1.5  $\mu\text{g}$  protein prepared as described above, were applied and air dried onto poly-L-lysine coated N.1.5 coverslips, fixed with 4% paraformaldehyde in PBS for 10 min at RT. Samples were incubated for 30 min in blocking solution (5% normal donkey serum, 0.3% BSA in PBS), followed by an incubation O/N at 4°C with primary antibodies in blocking solution and 1 h at RT with donkey anti-goat, donkey-anti rabbit and

donkey-anti guinea pig IgG (Jackson ImmunoResearch Europe Ltd, UK) conjugated with Alexa Fluor®594, ATTO 590 (ATTO-TEC GmbH, Siegen, Germany) or KK114 (kindly provided by Dr. V. Belov, Dept. of Nano Biophotonics, Max Planck Institute for Biophysical Chemistry) respectively, that were diluted 1:400 (Alexa Fluor®594) and 1:30 respectively (ATTO 590, KK114) in blocking solution. After washing with PBS, the coverslips were mounted onto glass slides using Mowiol. STED images were acquired using a custom-built stimulated emission depletion microscope which design has been described in detail before (13, 14). The STED microscope was based on a customized supercontinuum laser (SC-450-PP-HE, Fianium Ltd., Southampton, UK) with an applied repetition rate of 1 MHz and pulse width of approximately 100 ps. The excitation and STED beams were coupled together using dichroic mirrors (EXC1/STED1 z690SPRDC and EXC2/STED2 z655DCSPXR, Chroma Technology Corp., Bellow Falls, USA) before being sent into the microscope objective. The samples were placed on a three-dimensional scanning piezo stage coupled to a closed loop controller unit (MAX311/M and BPC203, Thorlabs, Sweden AB) offering a positional resolution of 5 nm. The fluorescence was collected back through the objective and separated from the excitation and the STED beams by a customized dichroic mirror (Laseroptik, Garbsen, Germany); The dual-color acquisition (pulsed interleaved by 40 ns) is routed through a time-delay and synchronization unit (P400 Digital delay generator, Highland Technology, San Francisco) allowing time-selective quasi-simultaneously recording of the two color channels while efficiently reducing imaged (color) cross-talk (14). The image size was set to 5 x 5  $\mu\text{m}^2$  with a pixel size of 20 nm for the STED images and 50 nm for the confocal images. Average applied powers were 1  $\mu\text{W}$  for both excitation beams, 2.2 mW and 1.2 mW for the two STED beams respectively.

### **Proximity Ligation Assay**

Samples for Duolink In situ Fluorescence Proximity Ligation Assay (PLA®, Olink Bioscience, Uppsala, Sweden) were prepared as described for STED microscopy. After primary antibody incubation, the PLA was performed according to the manufacturer's instruction. When the target proteins are in close proximity (<40 nm), for this purpose to detect possible vesicular co-localization, hybridization of the oligonucleotide arms of the PLA probes (PLUS and MINUS) will provide template for rolling circle amplification. As negative controls, none or only one primary antibody was used together with the PLA probes for dual detection (PLA

PLUS or MINUS). As positive controls, only one primary antibody was used together with PLA PLUS and MINUS probes against the same species as the primary antibody was raised in. PLA signals from 5 fields of view (75 x 75  $\mu\text{m}$ ) were quantified for each experiment. Documentation of fluorescent PLA signal was performed using a ZEISS LSM 510 META confocal microscope, a Plan-Apochromat 40x/1.4 NA oil immersion objective (ZEISS) and ZEISS LSM510 image analysis software.

### **Reverse Transcription-Quantitative PCR (RT-qPCR)**

RNase free environment was maintained throughout the experiment till cDNA synthesis. RNA isolated in TRI reagent (Ambion, Life Technologies) from mid brain (enriched in substantia nigra and ventral tegmental area), and striatum (enriched in caudate putamen and nucleus accumbens) was subjected to DNase I treatment (Fisher Scientific, Göteborg, Sweden). Treated RNA was again purified with TRI reagent, purity and integrity was checked on agarose gel. One  $\mu\text{g}$  of treated RNA was taken for cDNA synthesis by M-MLV reverse transcriptase (Invitrogen, Life Technologies). Primers were designed using Primer3 Plus software (<http://www.bioinformatics.nl/cgi-bin/primer3plus/primer3plus.cgi>) from adjacent exons in a gene wherever possible to avoid any contaminating amplification from traces of genomic DNA; verified by *in silico* PCR (<http://genome.ucsc.edu/cgi-bin/hgPcr?command=start>) taking mouse genome assembly released in Dec. 2011 (GRCm38/mm10) and using UCSC genes as template. Primers were also verified using cDNA from a wild type brain as template for optimal annealing temperature and single amplicons. Real time PCR was carried out on duplicate samples from wild type ( $n = 12$ ) and SLC10A4 null mutant mice ( $n = 12$ ) cDNAs using KAPA™ SyBr® FAST qPCR Kit (KAPA Biosystems Inc., Woburn, USA) and Bio-Rad iCycler™ (Bio-Rad). PCR efficiencies of primer pairs were calculated by linear regression method (downloaded from <http://www.hartfaalcentrum.nl/index.php?main=files&sub=LinRegPCR>). Cq values thus obtained were normalized to the geometric mean of three most stable reference genes, *Actb*, *Gapdh* and *Rpl19*, out of five genes tested on geNorm algorithm (<http://medgen.ugent.be/~jvdesomp/genorm/>). Final comparison between normalized Cq values of wild type and SLC10A4 null mutant samples was plotted on graph using GraphPad Prism©. List of primers used for RT-qPCR is given in the table below.

**Table S4. Primers for RT-qPCR**

Gene	Sequence	Tm	cDNA (bp)	gDNA (bp)	Gene Name
<i>Slc10a4_F</i>	GGATAGCATTGCATCGTCAAAC	60	110	110	Solute carrier family 10 member 4
<i>Slc10a4_R</i>	ACCCCTGGACAATGTTGATG				
<i>DIR_F</i>	TTCTCCTTTTCGCATCCTCAC	60	101	101	Dopamine receptor 1
<i>DIR_R</i>	TGTCGAAACCTGATGACAGC				
<i>D2R_F</i>	GAGAAGGCTTTGCAGACCAC	60	202	4037	Dopamine receptor 2
<i>D2R_R</i>	TGATGGCACACAGGTTCAAG				
<i>DAT_F</i>	TGGAGGTTTCCCTACCTGTG	60	144	2187	Dopamine active transporter
<i>DAT_R</i>	GACACCAGCAGCTCCTTCTC				
<i>TH_F</i>	CGAGGAGAGGGATGGAAATGC	61.3	82	82	Tyrosine hydroxylase
<i>TH_R</i>	CAAAGCCCGAGACAGTGAGG				
<i>Actb_F</i>	GATCTGGCACCACACCTTCT	60	209	663	Actin beta
<i>Actb_R</i>	CCATCACAATGCCTGTGGTA				
<i>Rpl19_F</i>	AATCGCCAATGCCAACTC	60	85	85	Ribosomal protein L19
<i>Rpl19_R</i>	GGAATGGACAGTCACAGG				
<i>Gapdh_F</i>	GCCTTCCGTGTTCTTACC	60	101	101	Glyceraldehyde-3-phosphate hydrogenase
<i>Gapdh_R</i>	GCCTGCTTCACCACCTTC				
<i>Tubb_F</i>	AGTGCTCCTCTTCTACAG	55	158	158	Tubulin beta
<i>Tubb_R</i>	TATCTCCGTGGTAAGTGC				
<i>Ppia_F</i>	TTTGGGAAGGTGAAAGAAGG	60	158	158	Peptidylprolyl isomerase A
<i>Ppia_R</i>	ACAGAAGGAATGGTTTGATGG				

### HEK-293 Uptake Studies

HEK293-hDAT-hVMAT2 cells were generously supplied by Dr. Aaron Janowsky (Oregon Health & Science University, Portland, USA) and Dr. Robert Edwards (University of California, San Francisco, USA). HEK-293 (passage number between 10 and 20) were maintained in Dulbecco's modified Eagle's medium supplemented with 10% fetal bovine serum and penicillin/streptomycin and grown in culture flasks at 5% CO<sub>2</sub>-95% air at 37°C. HEK293-hDAT-hVMAT2 were maintained in media supplemented with Genetecin (Invitrogen).

For ligand uptake/binding assays cells were plated in poly-L-lysine-coated coated 48-well culture plates and transfected the following day using Lipofectamine LTX (Invitrogen, Life Technologies, Carlsbad, USA) according to manufacturer's protocol. Transfection was verified using immunohistochemistry, western blot and pCMV6-YFP control vector, resulting in a transfection efficiency of approximately 50%. Human Slc10a4 cDNA vector (pCMV6-XL5, SC123272) was obtained from OriGene (OriGene, Rockville, MD, USA). Mock transfections

were used as controls (treatment with Lipofectamine reagents without addition of DNA) and cells in the same plate and with same confluency were compared.

Uptake studies were performed at 100% confluence, ca 48 h post transfection. The media was aspirated and the cells were washed once with 37°C PBS. [3H]-radio labeled compounds; dopamine (NET1160001MC, 74.5 Ci/mmol), serotonin (45.9 Ci/mmol, NEC225) and acetylcholine (ACh; NET113001MC, 73.1 Ci/mmol) were incubated at a concentration of 1 µCi/ml (approximately 100 nM), (Perkin Elmer, Waltham, Massachusetts, U.S.), diluted in PBS, and were incubated with the cells in 48-well plates for 15 minutes at 37°C (150 µl/well). For inhibition studies 10 µM amphetamine, 10 µM cocaine or 1 µM reserpine in PBS were pre-incubated for 5 minutes prior to uptake and included in the uptake solution. The assays were also performed on ice for background evaluation. The uptake was stopped by rapid aspiration of the uptake solution followed by two 5 minutes washes in PBS. Cells were lysed and the radioactivity remaining in each well was determined by liquid scintillation spectrometry in a Tri-Carb Liquid Scintillation Analyzer (Perkin Elmer), counts per minute average (CPMA) were used for comparison. Uptakes (CPMA) were normalized and expressed as percent of HEK293-hDAT-hVMAT2 Mock control. For HEK293 dopamine studies we performed 5 experiments with 17 individual wells ( $n = 17$ , 5 experiments), serotonin ( $n = 9$ , 3 experiments) and acetylcholine ( $n = 9$ , 3 experiments), HEK293-hDAT-hVMAT2 dopamine ( $n = 12$ , 4 experiments), HEK293-hDAT-hVMAT2 inhibition studies ( $n = 6$ , 2 experiments). Statistical significance was tested with Student's two-tailed *t*-test.

### **Monoamine and Acetylcholine Measurement**

High-performance liquid chromatography with electrochemical detection was performed to measure levels of DA, 5-HT and NA and DA metabolites, dihydroxyphenylacetic acid and homovanillic acid in nucleus accumbens and caudate putamen. Samples were collected from SLC10A4 null mutant and control mice ( $n = 20$ , 10 males and 10 females, homozygous breeding), dissected on ice and stored at -80°C prior to analysis. Samples were weighed and homogenized in 4% (w/v) cold perchloric acid containing 3,4-dihydroxybenzylamine as internal standard. Measurements were conducted as previously described (15).

The amount of choline and ACh from brain tissue was determined using a commercially available kit (ab65345, Abcam). Striatum and midbrain were rapidly dissected from SLC10A4

KO and control mice ( $n = 10$ , 4 males and 6 females, homozygous breeding), homogenized in assay buffer and stored on dry ice prior to measurement. Fluorescent measurements (Ex 535 nm/Em 590 nm) were performed using a Tecan Infinite M200 instrument (Tecan Group Ltd., Männedorf, Switzerland) and the ACh content was determined after acetylcholinesterase treatment by subtracting free choline from total content.

### **Chronoamperometric *in vivo* Measurement of Dopamine Release, Reuptake and Clearance**

Chronoamperometric recordings were performed using the Fast Analytical Sensing Technology (Quanteon LLC, Nicholasville, USA) according to methodological principles described previously (16). In short, single carbon fiber electrodes (30  $\mu\text{m}$  outer diameter, 100–200  $\mu\text{m}$  length; Quanteon) were coated with three layers of Nafion 5% solution (Sigma Aldrich) before use to prevent interference from anionic compounds such as ascorbic acid. Electrodes were then tested for sensitivity to ascorbic acid (250  $\mu\text{M}$ ) and calibrated with three accumulating concentrations of DA (2–6  $\mu\text{M}$ ) *in vitro*. Electrodes displaying selectivity ratios exceeding 500:1 over ascorbic acid and linear response to DA ( $R^2 > 0.995$ ) were used for *in vivo* experiments. Reduction/oxidation ratios (redox ratios) were calculated at the peak of every response to confirm the identity of the analyte contributing to the electrochemical signal. DA typically displays a redox ratio of 0.7 – 0.9 *in vivo*, whereas possible interfering electrochemical species have lower redox ratios (17). To ensure that DA was the contributor to the electrochemical signal, only experiments displaying redox ratios exceeding 0.7 were included in the data analysis. Urethane-anesthetized mice were placed in a stereotaxic frame and maintained at a body temperature of 37°C. The recordings were performed in the striatum (level: anterior-posterior, +1.1; medial-lateral, 1.5; dorsal-ventral, -3.2 in mm from Bregma). Stereotaxic coordinates were determined according to a standard brain atlas (18).

Chronoamperometric *in vivo* measurements of exogenous dopamine were performed to evaluate DA clearance in SLC10A4 null mutant mice ( $n = 6$ ) and littermate controls ( $n = 4$ ). For all recordings, 200  $\mu\text{M}$  of exogenous dopamine (Sigma-Aldrich) was used. DA was pressure-ejected at 5-min intervals into the striatum. By regulating the pressure (5-20 psi) and duration (0.3-0.5) of the injection volume, at least two consecutive amplitudes of each 5, 22 and 45  $\mu\text{M}$  were recorded. The mean values of each amplitude pairs were used for statistical analyses. The following parameters were analyzed: peak area (in  $\mu\text{M}\times\text{sec}$ ), T-rise (time between ejection and

maximum peak concentration), T-80 (the time from maximum peak concentration until 80% decrease of the maximum amplitude) and clearance rate Tc (Tc is defined as the change in amplitude between T20 and T60 divided by the change in time between T20 to T60, in  $\mu\text{M/s}$ ).

Chronoamperometric *in vivo* recordings of induced DA release were measured in SLC10A4 null mutant mice ( $n = 5$ ) and littermate controls ( $n = 5$ ). DA release was evoked by five consecutive pressure ejections of 120 mM KCl, applied locally at 5 min intervals as previously described (19). The following five parameters of the electrochemical signal were analyzed: 1) amplitude, defined as the peak DA concentration (micromoles) from baseline, 2) peak area (in  $\mu\text{M}\times\text{sec}$ ), 3) T-rise, time (s) between ejection and maximum peak concentration; 4) T-80, the time (s) from maximum peak concentration until 80% decrease of the maximum amplitude, and 5) clearance rate Tc (Tc is defined as the change in amplitude between T20 and T60 divided by the change in time between T20 to T60, in  $\mu\text{M/s}$ ) as a measure of DA clearance (20-22).

*Post Reserpine Experiments.* Chronoamperometric *in vivo* measurements of exogenous dopamine clearance and induced DA release and reuptake were measured in SLC10A4 null mutant mice ( $n = 3$ ) and controls ( $n = 4$ , respectively) in a similar manner using the same protocols as mentioned above. Reserpine was administered intraperitoneal (i.p.) at a concentration of 4 mg/kg 1 to 4 hours prior to chronoamperometric measurements.

Data were analyzed using two way ANOVA followed by Bonferroni *post-hoc* test.

### **Basal Behavioral Analysis**

Basal behavior analysis was performed on 10 SLC10A4 null mutant mice and 10 littermate controls (4 female and 6 males in each group) unless otherwise stated. During the different tests all SLC10A4 null mutant mice were housed together with their specific control and all animals had *ad libitum* access to food and water.

*Hanging wire* test was used to assess muscular strength. Each mouse was placed so that its forepaws could grab a rounded steel wire (2 mm thick), elevated 30 cm above the home cage. Four behaviors were noted and graded: entering the hind paw to the wire (1 p), hanging with a loose grip (2 p), never entering the steel wire (3 p) and falling off the wire (4 p). The muscle strength score thus spanned between 1 and 10, a value used for statistical analysis. Each mouse was tested three times the same day at 15 min intervals. Animals that jumped off the wire were

excluded from the trial (one mouse in trial 1, two mice in trial 2 and one mouse in trial 3).

*Rotarod* (Iitc Life Science, Woodland Hills, USA) was used to measure motor coordination and balance. The rotarod was set to accelerate from 3 to 40 rpm over 5 min. The mice were tested for three days and three trials were conducted each day. For each trial, the time and rpm were noted, and an average from the three trials on each day was used for statistical analysis.

The *elevated plus maze (EPM)* was used to measure anxiety-like behavior in mice. Each mouse was placed in the center of the EPM facing an open arm and the movements were recorded for 10 min. The following parameters were scored: latency (s) to the first entry into an arm, the frequency and duration (s) of visits into the inner and outer open and closed arms as well as the center portion. To be scored as a visit, both hind limbs of an animal should have entered a section.

The *multivariate concentric square field* was used to analyze exploration, risk assessment, risk taking, shelter seeking, approaching and avoidance behavior. In the same trial, the animal was exposed to a free choice of different environmental settings and items. This test and the functional interpretation of the various parameters generated were performed as earlier described (2; 23).

*Forced swimming test (FST)* was used to test depression-like behavior. Each mouse was placed in a glass cylinder (19 cm diameter, 35 cm high) containing 25°C water at a height of 20 cm and the behavior was monitored for 6 minutes. The period spent immobile was defined as time spent floating or making occasional paddling movements. The animals were introduced to the experimental set up for 6 minutes one day before the FST day. Each animal was analyzed in a random order, with changed water between animals and scored blindly. After experiments the mice were allowed to dry in a warm environment.

*Basal activity* of different locomotor-associated behaviors was measured simultaneously during 40 min in an automated device developed for activity monitoring, Locobox© cages (55 x 55 x 22 cm, Kungsbacka Reglerteknik AB, Sweden). The Locobox© cages were used for registration of various activities; horizontal activity, peripheral activity, locomotion, rearing activity, peripheral rearing (quantified as beam breaks) and rearing time and corner time (quantified in seconds). All those behavior activities were used for statistical comparison on SLC10A4 null mutant mice and littermate control ( $n = 44/\text{genotype}$ , equal numbers of males and

females in each group).

### **Behavior Analysis with Pharmacological Treatments**

*Drugs.* Cocaine and amphetamine (Apoteket Farmaci, Sweden), SKF 81297 and quinpirole (Tocris Biosciences) were diluted in saline and reserpine (Sigma-Aldrich) was dissolved in 20 µl acetic acid before diluted to the desired concentration with distilled water. GBR12783 and tranylcypromine (Tocris Biosciences) were dissolved in DMSO and then diluted with saline to obtain 5% DMSO/saline solutions.

*Drug induced-locomotor activity.* Adult SLC10A4 null mutant mice and their littermate controls were used as described in the section for *basal behavioral analysis* having equal numbers of males and females in each group. For amphetamine three doses were evaluated (0.5 mg/kg, 1.5 mg/kg and 3 mg/kg) on 28 animals per genotype (SLC10A4 null mutant and littermate control mice). Three different concentrations were used for cocaine (10, 20 and 30 mg/kg), GBR12783 (5, 10 and 15 mg/kg) and tranylcypromine (10, 15 and 20 mg/kg) on 16 mice per genotype for each respective drug. For reserpine, two doses (2 and 4 mg/kg) were administered to 16 mice per genotype and SKF 81297 (5 mg/kg) and quinpirole (2.5 mg/kg) to 9 mice per genotype. Animals were injected with vehicle only (saline or DMSO/saline) one day prior to first drug injections. For testing the effects of all different drugs, basal locomotor activity was measured for 30 minutes using Locoboxes© prior to i.p. injection of the respective drug or vehicle. Immediately after administration of vehicle or drug the animals were placed in the Locobox© again.

Changes in locomotor activity were measured for additional 60 min (for vehicle control injections using saline and 5% DMSO in saline) and 120 or 180 minutes, respectively (see Figure 6 and Figure S3). Dose-dependent change of locomotion for all drugs was investigated both in wild type and SLC10A4 KO mice using two to three different doses administered as 10 ml/kg (i.p.) (see Figure S3). Besides locomotion several other parameters like horizontal activity, peripheral activity, rearing activity, peripheral rearing, rearing time and corner time were recorded and analyzed for genotype specific differences. Data were analyzed using two-way ANOVA followed by Bonferroni *post-hoc* test.

*Reserpine induced catalepsy.* The effect of reserpine (2 mg/kg, i.p.) on 10 SLC10A4 null mutant and 10 control male mice was investigated by measuring cataleptic induced behavior and

activity in the Locobox<sup>®</sup>. Mice were positioned with their forepaws on a 3 cm high, 0.5 cm wide horizontal bar and the time was scored until they removed the forepaws from the bar, with a maximum cut-off time of 3 min. Scoring started 1 h after drug administration and was performed in 15 min intervals for 3 h. Directly after each catalepsy measurement, activity was recorded for 10 min in the Locobox<sup>®</sup>.

### **SLC10A4 Expression in Human Brain Autopsy Samples**

The human brain samples assessed here were obtained from a cognitively unimpaired female, age at death 81 years who died of cardiac arrest (Kuopio University Hospital, Eastern University Brain bank). The autopsy was carried out with consent and the study of the brain tissue was approved by National Authority for Medicolegal Affairs (# 60/04/044/07) in Finland. The research protocol regarding the human tissue was approved by the ethical committee of the Kuopio University Hospital. The postmortem delay was 104 hours. Shortly, the neuroanatomical regions assessed here including nucleus basalis of Meynert, substantia nigra, locus coeruleus and raphe nucleus did not display any of the common age related degenerative lesions such as hyperphosphorylated tau,  $\alpha$ -synuclein or  $\beta$ -amyloid pathology. The brain was placed in 10% buffered formaldehyde for one week, cut in to 1 cm thick coronal slices and embedded in paraffin. The 7- $\mu$ m-thick brain sections were manually stained. After deparaffinization and rehydration the endogenous peroxidase activity was quenched by incubation in 3% H<sub>2</sub>O<sub>2</sub> for 20 minutes. The sections were heat pretreated in 0.01M citrate buffer in microwave and incubated in +4°C overnight with the primary antibody diluted 1:500 (SIGMA SLC10A4). The reaction product was visualized using a PowerVision+ Poly-HRP detection kit (Immunovision Technologies, Daly City, CA), and Romulin 3-amino-9-ethylcarbazole as the chromogen (Biocare Medical, Walnut Creek, CA). Negative control staining with the omission of primary Abs revealed no detectable staining. A membrane with absorbed human brain proteins (ProSci Inc., Poway, USA) were obtained for western blot analyses. Western blot procedure was conducted as earlier described.

### **Statistical Analysis**

Statistical analyses were performed using GraphPad Prism (GraphPad Software, La Jolla, USA). ANOVA with Bonferroni's post hoc-test was used where applicable, otherwise Student's

two-tailed *t*-test. Outliers were determined using Grubbs test or GraphPad Quick Calcs with alpha = 0.05. Information about the statistical methods used for each experiment is stated in the Figure legends and in the Supplemental Methods & Materials section.

## Supplemental References

1. Takamori S, Holt M, Stenius K, Lemke EA, Grønberg M, Riedel D, *et al.* (2006) Molecular anatomy of a trafficking organelle. *Cell* 127(4):831-46.
2. Meyerson BJ, Augustsson H, Berg M Roman E (2006). The Concentric Square Field: a multivariate test arena for analysis of explorative strategies. *Behav Brain Res* 168:100-113.
3. Mucke L, Masliah E, Johnson WB, Ruppe MD, Alford M, Rockenstein EM, *et al.* (1994). Synaptotrophic effects of human amyloid beta protein precursors in the cortex of transgenic mice. *Brain Res* 666:151–167.
4. Amilhon B, Lepicard E, Renoir T, Mongeau R, Popa D, Poirel O, *et al.* (2010) VGLUT3 (vesicular glutamate transporter type 3) contribution to the regulation of serotonergic transmission and anxiety. *J Neurosci.* 30(6):2198-210.
5. Geyer J, Fernandes CF, Döring B, Burger S, Godoy JR, Rafalzik S, *et al.* (2008). Cloning and molecular characterization of the orphan carrier protein Slc10a4: expression in cholinergic neurons of the rat central nervous system. *Neuroscience.* 152(4):990-1005.
6. Enjin A, Rabe N, Nakanishi ST, Vallstedt A, Gezelius H, Memic F, *et al.* (2010). Identification of novel spinal cholinergic genetic subtypes disclose Chodl and Pitx2 as markers for fast motor neurons and partition cells. *J Comp Neurol.* 518(12):2284-304.
7. Schaeren-Wiemers and Gerfin-Moser, (1993). A single protocol to detect transcripts of various types and expression levels in neural tissue and cultured cells: in situ hybridization using digoxigenin-labelled cRNA probes. *Histochem.* 100(6):431-40.
8. Wang X, Herberg FW, Laue MM, Wullner C, Hu B, Petrasch-Parwez E, Kilimann MW (2000). Neurobeachin: A protein kinase A-anchoring, beige/Chediak-higashi protein homolog implicated in neuronal membrane traffic. *J Neurosci.* 20(23):8551-65.
9. Burry R, Vandr  DD, Hayes DM (1992). Silver enhancement of fold antibody probes in pre-embedding electron microscopic immunocytochemistry. *J Histochem Cytochem* 40:1849–1856.
10. Teng L, Crooks PA, Dwoskin LP (1998). Lobeline displaces [3H]dihydrotetrabenazine binding and releases [3H]dopamine from rat striatal synaptic vesicles: comparison with d-amphetamine. *J Neurochem.* 71(1):258-65.
11. Ahmed S, Holt M, Riedel D, Jahn R. (2013): Small-scale isolation of synaptic vesicles from mammalian brain. *Nat Protoc.* 8(5):998-1009.
12. Goh GY, Huang H, Ullman J, Borre L, Hnasko TS, Trussell LO, Edwards RH (2011). Presynaptic regulation of quantal size: K<sup>+</sup>/H<sup>+</sup> exchange stimulates vesicular glutamate transport. *Nat Neurosci.* 14(10):1285-92.
13. Wildanger D, Rittweger E, Kastrop L, Hell SW (2008). STED microscopy with a supercontinuum laser source. *Opt Express.* 16(13):9614-21.
14. Neumann D, Bückers J, Kastrop L, Hell SW, Jakobs S (2010). Two-color STED microscopy reveals different degrees of colocalization between hexokinase-I and the three human VDAC isoforms. *PMC Biophys.* 3(1):4.
15. Höglund E, Balm P, Winberg S (2000). Skin darkening, a potential social signal in subordinate arctic charr (*Salvelinus alpinus*): the regulatory role of brain monoamines and pro-opiomelanocortin-derived peptides. *J Exp Biol.* 203:1711-1721.
16. Gerhardt GA, Burmeister JJ (2000). Voltammetry in vivo for chemical analysis of the nervous system. In: *Encyclopedia of analytical chemistry* (Meyers RE, ed), pp 710–731.

17. Gerhardt GA, Hoffman AF (2001). Effects of recording media composition on the responses of Nafion-coated carbon fiber microelectrodes measured using high-speed chronoamperometry. *J Neurosci Methods* 109:13–21.
18. Franklin K, Paxinos G (2008). *The mouse brain in stereotaxic coordinates*, 3<sup>rd</sup> ed. New York: Academic Press.
19. Alsjö J, Nordenankar K, Arvidsson E, Birgner C, Mahmoudi S, Halbout B, *et al.* (2011) Enhanced sucrose and cocaine self-administration and cue-induced drug seeking after loss of VGLUT2 in midbrain dopamine neurons in mice. *J Neurosci.* 31(35):12593-603.
20. Cass WA, Zahniser NR, Flach KA, Gerhardt GA (1993) Clearance of exogenous dopamine in rat dorsal striatum and nucleus accumbens: role of metabolism and effects of locally applied uptake inhibitors. *J Neurochem* 61:2269–2278.
21. Hebert MA, Van Horne CG, Hoffer BJ, Gerhardt GA (1996). Functional effects of GDNF in normal rat striatum: presynaptic studies using in vivo electrochemistry and microdialysis. *J Pharmacol Exp Ther* 279: 1181–1190.
22. Hoffman AF, Lupica CR, Gerhardt GA (1998). Dopamine transporter activity in the substantia nigra and striatum assessed by high-speed chronoamperometric recordings in brain slices. *J Pharmacol Exp Ther* 287:487–496.
23. Wallén-Mackenzie A, Nordenankar K, Fejgin K, Lagerström MC, Emilsson L, Fredriksson R, *et al.* (2009). Restricted cortical and amygdaloid removal of vesicular glutamate transporter 2 in preadolescent mice impacts dopaminergic activity and neuronal circuitry of higher brain function. *J Neurosci.* 29(7):2238-51.